Article

A New Family of Weighted T-X Distributions with Environmental Health and Textile Engineering Applications

Gabriel O. Orji[1], Harrison O. Etaga[2] and Okechukwu J. Obulezi[3,*]

[1] Department of Statistics, Faculty of Physical Sciences, Nnamdi Azikiwe University, P. O. Box 5020, Awka, Nigeria.; go.orji@unizik.edu.ng
[2] Department of Statistics, Faculty of Physical Sciences, Nnamdi Azikiwe University, P. O. Box 5020, Awka, Nigeria.; ho.etaga@unizik.edu.ng
[3] Department of Statistics, Faculty of Physical Sciences, Nnamdi Azikiwe University, P. O. Box 5020, Awka, Nigeria.; oj.obulezi@unizik.edu.ng
* Correspondence: oj.obulezi@unizik.edu.ng

Abstract

This study presents a novel framework for modeling fine particulate matter (PM2.5) hazards and the tensile strength of polyester, using a newly formulated family of weighted T-X distributions, termed the Odd Reparametrized Exponential Transformed-X (ORET-X) family. With growing concerns over the health and environmental risks associated with PM2.5 exposure—particularly its link to respiratory and cardiovascular diseases—and the reliability challenges posed by polyester tensile strength, this work aims to offer a more flexible modeling approach for both fields. The ORET-X family builds upon the exponential distribution via reparametrization, introducing an odd function transformation to enhance the modeling of hazard functions and tail behavior. Specifically, the Odd Reparametrized Exponential Transformed-Lomax (ORET-L) distribution, a subclass of the ORET-X family, was developed and analyzed. The study utilized both Bayesian and non-Bayesian estimation methods, with results demonstrating improved model accuracy as sample sizes increased. Bayesian estimation showed reduced bias and lower Root Mean Squared Error (RMSE) across parameters, particularly at smaller sample sizes, underscoring the robustness of the parameter estimates. The ORET-X family offers significant promise in environmental health, engineering, and other domains requiring flexible hazard-based distributions. Our results suggest that the ORET-L model provides superior fit and predictive accuracy for modeling PM2.5 exposure mortality, as shown through various statistical performance metrics and visual assessments, making it a compelling tool for both environmental risk modeling and engineering applications.

Keywords: Bayesian estimation; environmental health risks; Odd Reparametrized Exponential Transformed-X (ORET-X); PM2.5 hazards; Tensile Strength of Polyester.

Received: March 10, 2025
Revised: April 21, 2025
Accepted: May 10, 2025
Published: June 26, 2025

Citation: Orji, Gabriel, Harrison Etaga, and Okechukwu Obulezi. 2025. A New Family of Weighted T-X Distributions with Environmental Health and Textile Engineering Applications. *Multi-Research* 1: 1. https://doi.org/10.32100/mr01

0. Introduction

Fine particulate matter (PM2.5) refers to tiny particles or droplets in the air that are less than 2.5 micrometers in diameter. To give a sense of scale, these particles are approximately 30 times smaller than the width of a human hair. Due to their small size, PM2.5 particles

can be easily inhaled into the lungs and even enter the bloodstream, which makes them a significant health risk. PM2.5 originates from a variety of sources, both natural and man-made. Among the most common man-made sources are vehicle emissions, which include pollutants from cars, trucks, and buses. Industrial processes, such as those from factories and power plants, also contribute to the concentration of PM2.5 in the atmosphere. The burning of fossil fuels, such as coal, oil, and gas, further exacerbates the production of these fine particles, ((Chowdhury et al. 2022; Seinfeld and Pandis 2016)). In addition, natural sources, such as wildfires and agricultural burning, as well as dust from construction activities and unpaved roads, contribute to the presence of PM2.5 in the air. Moreover, secondary particles can form in the atmosphere when gases like sulfur dioxide (SO_2) and nitrogen oxides (NO_x) react with other substances, ((Li et al. 2018)). The health effects associated with PM2.5 exposure are of serious concern. Due to their small size, these particles can penetrate deep into the respiratory system and affect vital organs such as the lungs and heart. Prolonged or chronic exposure to PM2.5 has been linked to a variety of health problems, including respiratory diseases like asthma and chronic obstructive pulmonary disease (COPD), ((Brook et al. 2010; Nolla Solé et al. 2012)). Cardiovascular diseases, such as heart attacks and strokes, are also more common among individuals exposed to high levels of PM2.5. Furthermore, long-term exposure to fine particulate matter can contribute to premature death, particularly among individuals who already suffer from heart disease or respiratory illnesses. Lung cancer and developmental effects in children are other significant health risks, ((Pope III and Dockery 2006)). Additionally, recent studies suggest that PM2.5 exposure may also have adverse effects on the nervous system, ((Calderón-Garcidueñas et al. 2002; Guttikunda et al. 2013)). Beyond the direct health impacts, PM2.5 also has a detrimental effect on the environment. The particles can reduce visibility, contributing to haze and smog, which in turn negatively affects air quality. PM2.5 can also settle on soil and water bodies, where it can harm ecosystems and vegetation. PM2.5 is typically measured in micrograms per cubic meter ($\mu g/m^3$). Monitoring the concentration of PM2.5 is essential for assessing air quality, as levels that exceed recommended thresholds indicate unhealthy air conditions. The measurement of PM2.5 plays a crucial role in public health and environmental protection efforts.

Similarly, tensile strength is a critical mechanical property that measures the maximum stress a material can withstand while being stretched or pulled before breaking (Agarwal, Broutman, and Chandrashekhara 2017; Hearle and Morton 2008). Polyester fibers, known for their durability, resistance to stretching, and versatility, are widely used in various industrial and textile applications (Bledzki and Gassan 1999; Okubo, Fujii, and Yamamoto 2004). Understanding the tensile strength of polyester fibers is essential for quality control, material selection, and ensuring performance reliability in different environments (Baley 2002). The observed tensile strength of polyester, as presented in this study, represents a dataset of real-world measurements aimed at evaluating the material's behavior under stress. These measurements provide valuable insights into the statistical properties and variability of polyester tensile strength, enabling the identification of suitable probabilistic models for its characterization. Such analyses play a vital role in optimizing polyester applications and ensuring compliance with industry standards (Agarwal, Broutman, and Chandrashekhara 2017; Hearle and Morton 2008).

Now, modeling life events such as the hazards associated with the fine particulate matter and the tensile strength of polyester using distributions has attracted great attention in the statistical literature over the last three decades. The reason is not far-fetched, the ability of such models to incorporate uncertainty of outcomes and explain random or unpredictable realities. While these become interesting, researchers have further enhanced the possibility of reproducing distributions through the construction of families of distributions

and generators of these families namely the popular $T - X$ generator by (Alzaatreh, Lee, and Famoye 2013). For brevity, we present in a table, some of the popular families of distributions, see Table (1) and discuss some resulting distributions from these families, see Table (2).

Table 1. Related Families of Distributions

Author	Family of Distributions
(Tahir et al. 2016)	Logistic-X family of distributions
(Elbatal et al. 2022)	odd-Perks-G family of distributions
(Cordeiro and De Castro 2011)	Kumaraswamy-G family of distributions
(Alzaatreh, Lee, and Famoye 2013)	T-X generator of families of continuous distributions
(Yousof et al. 2018)	Burr-Hatke-G family of distributions
(Maurya and Nadarajah 2021)	Poisson generated family of distributions
(Alizadeh, Cordeiro, Pinho, and Ghosh 2017)	The Gompertz-G family of distributions
(Hassan and Nassr 2019)	Power Lindley-G family of distributions
(Alzaatreh, Lee, and Famoye 2014)	T-normal family of distributions
(Gomes-Silva et al. 2017)	The odd Lindley-G family of distributions
(Al-Shomrani et al. 2016)	Toppâ€“Leone Family of Distributions
(Anzagra, Sarpong, and Nasiru 2022)	Odd Chen-G family of distributions
(Yousof et al. 2018)	Burr-Hatke-G family of distributions
(Oramulu et al. 2024)	Sine generalized family of distributions
(Cordeiro, Alizadeh, and Diniz Marinho 2016)	The type I half-logistic family of distributions
(Lehmann 2011)	Ordered families of distributions
(Jamal, Chesneau, and Elgarhy 2020)	Type II general inverse exponential family of distributions

Table 2. Distributions Associated with the Families in Table (1)

Author	Distributions
(Mansoor, Cordeiro, and Zubair 2020)	Logistic exponentiated-exponential distribution
(Ekemezie et al. 2024)	odd-Perks-Lomax distribution
(Bourguignon et al. 2013)	The kumaraswamy Pareto distribution
(Jafari and Tahmasebi 2016)	Gompertz-power series distributions
(Anyiam et al. 2024)	Topp-Leone Burr-Hatke-exponential distribution
(Alizadeh et al. 2018)	Exponentiated power Lindley power series class of distributions
(Tolba et al. 2023)	odd Lindley-Pareto distribution
(Elbatal and Elgarhy 2013)	Kumaraswamy quasi Lindley distribution
(Al-Marzouki, Jamal, Chesneau, and Elgarhy 2019)	Type II Topp Leone power Lomax distribution
(Almarashi, Badr, Elgarhy, Jamal, and Chesneau 2020)	half-logistic inverse Rayleigh distribution
(Alyami et al. 2022)	Topp–Leone modified Weibull distribution

The motivation for developing the Odd Reparametrized Exponential Transformed-X (ORET-X) family of distributions is rooted in the need for a more robust and flexible approach to modeling complex environmental hazards, particularly those associated with fine particulate matter (PM2.5). Given the profound health risks that PM2.5 poses—such as respiratory and cardiovascular diseases, as well as potential neurological impacts—a distribution family capable of capturing the nuanced behavior of PM2.5 concentrations across varying levels and exposure times is essential. Current distribution models, while effective, often lack the adaptability needed to accurately represent hazard functions and the unique tail behaviors associated with environmental pollutants like PM2.5. The ORET-X family addresses this by building upon the exponential distribution with a reparametrization and an odd function transformation, which enhances its flexibility for hazard-based applications. This modification allows the ORET-X family to account for both moderate and extreme pollutant levels, offering improved accuracy in modeling hazard rates and associated health risks. Furthermore, by incorporating Bayesian and non-Bayesian estimation methods, the ORET-X family not only achieves greater modeling precision but also improves parameter estimation stability across diverse sample sizes. This distribution family therefore holds significant promise for environmental health studies, providing a sophisticated statistical tool for examining and predicting the hazards of PM2.5 and similar environmental factors.

The rest of this article are presented in the sequence in the flowchart as detailed in Figure (1)

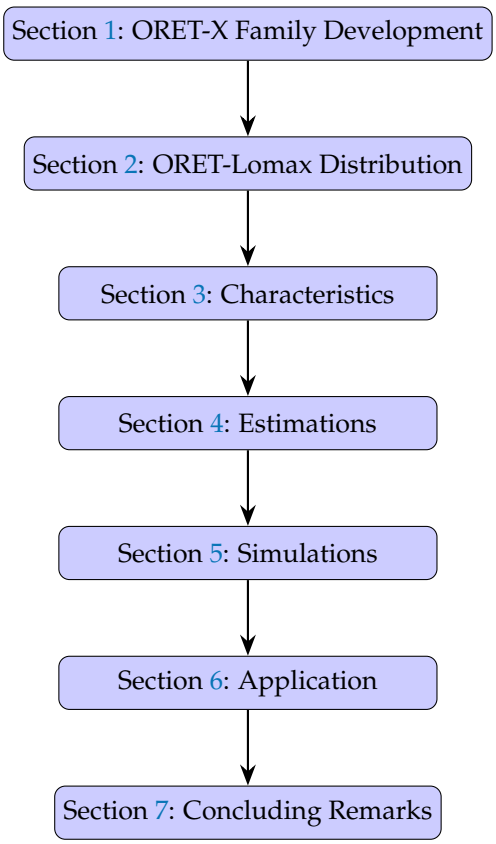

Figure 1. Flowchart of the sections of this article

1. Odd Reparametrized Exponential Transformed-X (ORET-X) Family of Distributions

In this study, we construct a new distribution from the exponential distribution by parametrization. The probability density function (PDF) of the reparametrized exponential distribution (RE) is $r(t) = \frac{\alpha}{e-1} e^{-\frac{\alpha t}{e-1}}, \quad t > 0$ with a new scale weight, $\frac{\alpha}{e-1}$. The cumulative distribution function (CDF) easily follows from the integration of $r(t)$ from zero up to a certain t, hence $R(t) = 1 - e^{-\frac{\alpha t}{e-1}}$. One can then write that $T \sim \text{RE}\left(\frac{\alpha}{e-1}\right)$. Next, we follow the argument of (Alzaatreh, Lee, and Famoye 2013), utilizing the odd function $W[G(x;\nabla)] = \frac{G(x;\nabla)}{1-G(x;\nabla)}$ as the generalizer in order to realized a new family of distributions, where $G(x;\nabla)$ is the CDF of any parent distribution. The CDF and PDF of the new family of distributions are expressed as

$$F(x;\alpha,\nabla) = \int_0^{\frac{G(x;\nabla)}{1-G(x;\nabla)}} r(t)\, dt = 1 - e^{-\frac{\alpha G(x;\nabla)}{(e-1)[1-G(x;\nabla)]}}, \tag{1}$$

and

$$f(x;\alpha,\nabla) = \frac{\partial W[G(x;\nabla)]}{\partial x} r\{W[G(x;\nabla)]\} = \frac{\alpha g(x;\nabla)}{(e-1)(1-G(x;\nabla))^2} e^{-\frac{\alpha G(x;\nabla)}{(e-1)[1-G(x;\nabla)]}}, \tag{2}$$

respectively. ∇ is the parameter vector for any parent distribution with CDF $G(x;\nabla)$. The hazard function $h(x;\nabla) = \frac{f(x;\alpha,\nabla)}{1-F(x;\alpha,\nabla)}$ is

$$h(x;\nabla) = \frac{\alpha g(x;\nabla)}{(e-1)(1-G(x;\nabla))^2}. \tag{3}$$

This new family is referred to as the "Odd Reparametrized Exponential Transformed-X " (ORET-X) family of distributions. Notice that $r(t)$ is a valid PDF and $\frac{G(x;\nabla)}{1-G(x;\nabla)}$ satisfies the criteria provided in the $T-X$ generator of family of distributions by (Alzaatreh, Lee, and Famoye 2013). That is, $\int_0^\infty \frac{\alpha}{e-1} e^{-\frac{\alpha t}{e-1}}\, dt = 1$ and

(a) $W\{G(x;\nabla)\} \in [a,b]$.

(b) W is differentiable and monotonically non-decreasing.

(c) $Z\{G(x;\nabla)\} \to a$ as $x \to -\infty$ and $W\{G(x;\nabla)\} \to b$ as $x \to \infty$,

where $[a,b]$ is the domain of the random variable T such that $-\infty \leq a < b \leq \infty$.

Introducing $\frac{1}{e-1}$ as a multiplier to the parameter of the exponential distribution effectively scales the parameter down by this constant factor. This change will influence the distribution in some key ways;

(i) The scaling effect on the mean: Since the mean of an exponential distribution with rate parameter α is $\frac{1}{\alpha}$, applying $\frac{1}{e-1}$ as a multiplier will increase the mean of the distribution by a factor of $e-1$. This makes the distribution more spread out compared to the original, effectively elongating the tail.

(ii) Shift in the hazard function: The hazard rate for the exponential distribution is constant and equal to α. With the new scaled parameter, this hazard rate is reduced by a factor of $e-1$. This makes the model more flexible for applications where the rate of occurrence of events decreases slightly over time, even while remaining relatively constant.

(iii) Impact on model fitting and interpretability: The added scaling factor allows the model to fit certain real-world data more closely, especially if the data demonstrates a slower rate of decay. The factor $\frac{1}{e-1}$ serves as a tuning parameter for how steeply the probability distribution falls off, affecting the fit quality and interpretatbility of the model parameters.

(iv) Normalization and Probability Constraints: Introducing this factor, ensures the modified model still maintains the properties of a probability distribution but slightly change the likelihood function. This impacts estimation procedures, as the parameter estimates will account for this scaling in the likelihood maximization process.

2. Odd Reparametrized Exponential Transformed-Lomax (ORET-L) Distribution

The Lomax distribution by (Lomax 1954), also known as the Pareto Type II distribution, is a heavy-tailed probability distribution widely used in fields such as business, economics, actuarial science, queueing theory, and internet traffic modeling. It's PDF and CDF are respectively given as $g(x;\beta,\lambda) = \frac{\beta}{\lambda}\left(1+\frac{x}{\lambda}\right)^{-\beta-1}$ and $G(x;\beta,\lambda) = 1-\left(1+\frac{x}{\lambda}\right)^{-\beta}; \quad x \geq 0$. The ORET-L distribution CDF and PDF are obtained by plugging back the $G(x;\beta,\lambda)$ and $g(x;\beta,\lambda)$ of Lomax distribution into equations (1) and (2). Thus;

$$F(x;\alpha,\beta,\lambda) = 1 - e^{-\frac{\alpha}{(e-1)}\left\{\left(1+\frac{x}{\lambda}\right)^{\beta}-1\right\}}; \quad x > 0, \tag{4}$$

and

$$f(x;\alpha,\beta,\lambda) = \frac{\alpha\beta}{\lambda(e-1)}\left(1+\frac{x}{\lambda}\right)^{\beta-1} e^{-\frac{\alpha}{(e-1)}\left\{\left(1+\frac{x}{\lambda}\right)^{\beta}-1\right\}}, \tag{5}$$

where $\beta > 0$ is the shape parameter and $\alpha > 0$ and $\lambda > 0$ are the scale parameters.

The hazard function of the ORET-L distribution is

$$h(x;\alpha,\beta,\lambda) = \frac{\alpha\beta}{\lambda(e-1)}\left(1+\frac{x}{\lambda}\right)^{\beta-1}. \tag{6}$$

The extreme behavior of the $h(x;\alpha,\beta,\lambda)$ in equation (6) depends primarily on the parameters β and λ, which influence how the distribution behaves as $x \to 0$ (considering lower bounds) and as $x \to \infty$ (considering upper bounds).

As $x \to 0$, the term $\left(1+\frac{x}{\lambda}\right)^{\beta-1}$ in the hazard function approaches 1. Consequently, $h(x;\alpha,\beta,\lambda)$ simplifies approximately to $\frac{\alpha\beta}{\lambda(e-1)}$, suggesting that the hazard function has a finite lower bound as $x \to 0$, which depends on the parameters α, β, and λ. This implies that the function does not approach zero or infinity as $x \to 0$; rather, it reaches a fixed value.

In contrast, as $x \to \infty$, the term $\left(1+\frac{x}{\lambda}\right)^{\beta-1}$ behaves differently depending on the value of β. Specifically, for $\beta > 1$, this term grows unbounded, causing $h(x;\alpha,\beta,\lambda)$ to increase towards infinity as $x \to \infty$. On the other hand, if $\beta < 1$, the term $\left(1+\frac{x}{\lambda}\right)^{\beta-1}$ diminishes towards zero, leading $h(x;\alpha,\beta,\lambda)$ to decay to zero as $x \to \infty$. This difference in behavior based on the value of β reveals distinct tail properties: when $\beta > 1$, the hazard has a heavier upper tail as it diverges at infinity, while for $\beta < 1$, it has a lighter tail, converging to zero as $x \to \infty$.

Therefore, the extreme behavior of $h(x;\alpha,\beta,\lambda)$ indicates that the hazard function may either grow unbounded or decay at large values of x based on the value of β. This distinction provides insight into the tail characteristics of the hazard function and how it may be applied to model data with varying degrees of tail weight.

Figure (2) contains the PDF of the ORET-L distribution with majorly positively skewed shape and reversed bathtub shape. Figures (3-6) are the plots of the hazard rate, which is traditionally used as a mortality indicator in survival analysis. The plots represent strictly decreasing, strictly increasing, L-shape and J-shape respectively.

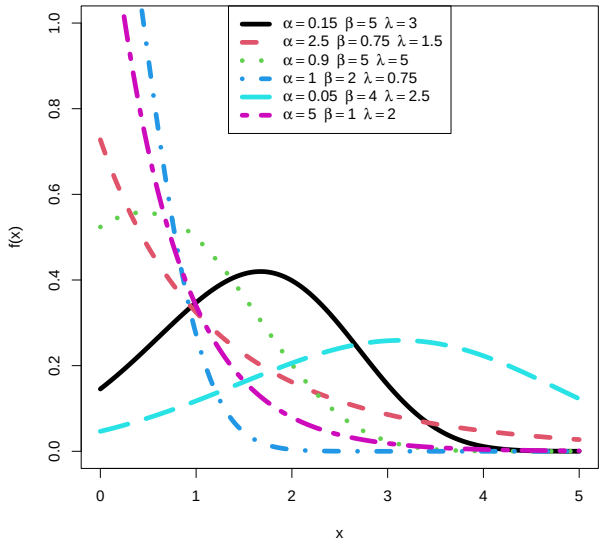

Figure 2. $f(x;\alpha,\beta,\lambda)$ of ORET-L

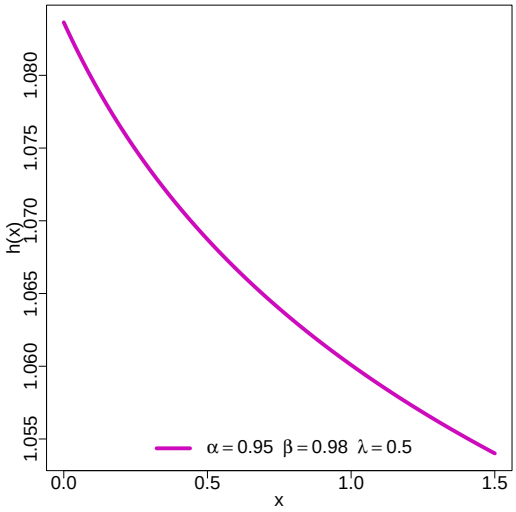

Figure 3. h(x) of ORET-L

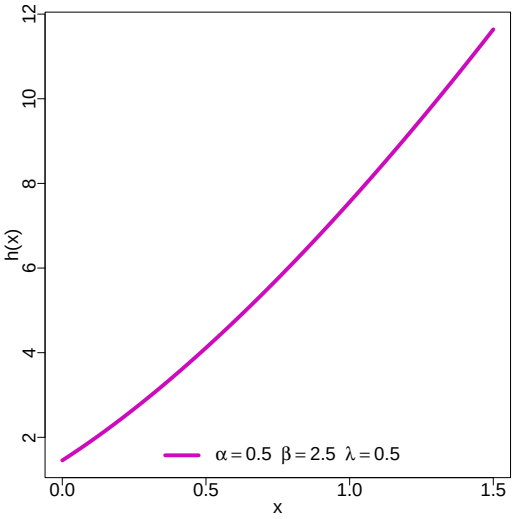

Figure 4. h(x) of ORET-L

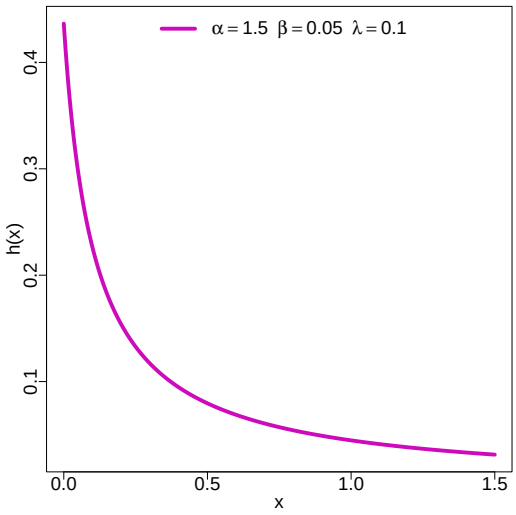

Figure 5. h(x) of ORET-L

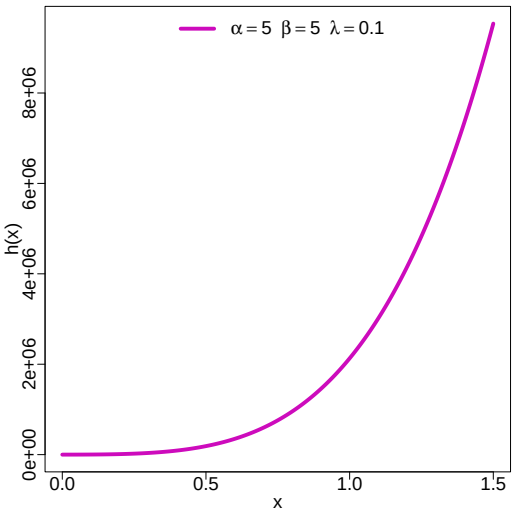

Figure 6. h(x) of ORET-L

3. Characteristics

Theorem 3.1 (Quantile Function and Value at Risk Measure). *The Value at Risk (VaR) is defined as the quantile corresponding to a specific confidence level, this quantile function directly serves as the VaR for that level. The quantile function for the ORET-L distribution at the confidence level p. When interpreting this quantile as the VaR at the same confidence level p, it directly becomes the VaR. In finance, you often use a lower tail, meaning the quantile for a high probability (e.g., 95% or 99% confidence), to represent the maximum expected loss.*

$$VaR_p = x_p = \lambda\left(\left(1 - \frac{(e-1)}{\alpha}\ln(1-p)\right)^{\frac{1}{\beta}} - 1\right). \tag{7}$$

This expression represents the VaR at a confidence level p, where x_p is the quantile at that level.

Theorem 3.2 (*s*-th Raw Moment). *The next important index is the s-th raw moment for the ORET-L distribution which is given as*

$$\mu_s' = \lambda^s e^{\frac{\alpha}{e-1}} \sum_{i=0}^{s} (-1)^i \binom{s}{i} \left(\frac{\alpha}{e-1}\right)^{\frac{i}{\beta}-\frac{s}{\beta}} \Gamma\left(\frac{s}{\beta} - \frac{i}{\beta} + 1\right); \quad where \quad s = 1, 2, \cdots \tag{8}$$

Proof. The s-th moment of a continuous random variable X is mathematically defined as $\mathbb{E}X^s = \int_0^\infty x^s f(x;\alpha,\beta,\lambda)\, dx$. When we introduce the PDF of the ORET-L distribution, the rest is trivial. □

Theorem 3.3 (Rény Entropy). *The Rény entropy for the ORET-L distribution is*

$$I_\theta = \frac{1}{1-\theta}\log\left\{\left(\frac{\beta}{\lambda}\right)^{\theta-1} e^{\frac{\alpha\theta}{e-1}}\left(\frac{\alpha\theta}{e-1}\right)^{\frac{\theta}{\beta}-\frac{1}{\beta}}\Gamma\left(\theta-\frac{\theta}{\beta}+\frac{1}{\beta}\right)\right\}, \tag{9}$$

for $\theta \neq 1$ and $\theta > 0$.

Corollary 3.4. *When $\theta \to 1$, a special entropy by (Shannon 1948) is obtained.*

Proof. Let's proceed by applying L'Hôpital's Rule in detail. This involves differentiating the numerator and the denominator with respect to θ and then evaluating the limit as $\theta \to 1$.

$$\lim_{\theta\to 1} I_\theta = \lim_{\theta\to 1} \frac{\log\left(\left(\frac{\beta}{\lambda}\right)^{\theta-1} e^{\frac{\alpha\theta}{e-1}}\left(\frac{\alpha\theta}{e-1}\right)^{\frac{\theta}{\beta}-\frac{1}{\beta}}\Gamma\left(\theta-\frac{\theta}{\beta}+\frac{1}{\beta}\right)\right)}{1-\theta}.$$

Expand the Logarithm

$$\log\left\{\left(\frac{\beta}{\lambda}\right)^{\theta-1}\right\} = (\theta-1)\log\left(\frac{\beta}{\lambda}\right), \quad \log\left(e^{\frac{\alpha\theta}{e-1}}\right) = \frac{\alpha\theta}{e-1},$$

$$\log\left\{\left(\frac{\alpha\theta}{e-1}\right)^{\frac{\theta}{\beta}-\frac{1}{\beta}}\right\} = \left(\frac{\theta}{\beta}-\frac{1}{\beta}\right)\log\left(\frac{\alpha\theta}{e-1}\right), \quad \text{and} \quad \log\left(\Gamma\left(\theta-\frac{\theta}{\beta}+\frac{1}{\beta}\right)\right).$$

So, we have:

$$\begin{aligned}
&\log\left\{\left(\frac{\beta}{\lambda}\right)^{\theta-1} e^{\frac{\alpha\theta}{e-1}}\left(\frac{\alpha\theta}{e-1}\right)^{\frac{\theta}{\beta}-\frac{1}{\beta}}\Gamma\left(\theta-\frac{\theta}{\beta}+\frac{1}{\beta}\right)\right\}\\
&= (\theta-1)\log\left(\frac{\beta}{\lambda}\right) + \frac{\alpha\theta}{e-1} + \left(\frac{\theta}{\beta}-\frac{1}{\beta}\right)\log\left(\frac{\alpha\theta}{e-1}\right)\\
&+ \log\left(\Gamma\left(\theta-\frac{\theta}{\beta}+\frac{1}{\beta}\right)\right).
\end{aligned}$$

Differentiating each term in the numerator with respect to θ and applying L'Hôpital's Rule, product rule, and for $\log\left(\Gamma\left(\theta-\frac{\theta}{\beta}+\frac{1}{\beta}\right)\right)$, the derivative of $\log\Gamma(x)$ as $\psi(x)$, we get $\psi\left(\theta-\frac{\theta}{\beta}+\frac{1}{\beta}\right)\left(1-\frac{1}{\beta}\right)$. When $\theta = 1$, this term simplifies to $\psi\left(\frac{1}{\beta}\right)\left(1-\frac{1}{\beta}\right)$. The limit of I_θ as $\theta \to 1$ is then:

$$\lim_{\theta\to 1} I_\theta = \log\left(\frac{\beta}{\lambda}\right) + \frac{\alpha}{e-1} + \frac{1}{\beta}\log\left(\frac{\alpha}{e-1}\right) + \psi\left(\frac{1}{\beta}\right)\left(1-\frac{1}{\beta}\right).$$

This is the limiting value of I_θ as $\theta \to 1$. □

Theorem 3.5 (Distribution of the k-th Order Statistic)**.** *The distribution of the k-th order statistic for the ORET-L distribution is*

$$f_{X_{(k)}}(x) = \frac{\alpha\beta n!}{(k-1)!(n-k)!\lambda(e-1)} \sum_{j,l=0}^{\infty} \sum_{h,n=0}^{\infty} \sum_{m=0}^{l} \sum_{p=0}^{l+h+n} \sum_{q=0}^{\beta(l+h+n-p)+\beta-1} \frac{j^n(-1)^{j+l+h+m+n+p}}{l!h!n!}$$
$$\times \binom{k-1}{j}\binom{l}{m}\binom{l+h+n}{p}\binom{\beta(l+h+n-p)+\beta-1}{q}\left(\frac{\alpha}{e-1}\right)^{l+h+n}$$
$$\times k^m n^{l-m}\left(\frac{x}{\lambda}\right)^q.$$

Theorem 3.6 (The Moment Generating Function (MGF))**.** *The MGF of the random variable X which is the ORET-L distributed written as $M_X(t)$ can be defined as*

$$M_X(t) = \mathbb{E}(e^{Xt}) = \lambda^r e^{\frac{\alpha}{e-1}} \sum_{r=0}^{\infty} \sum_{i=0}^{r} \frac{(-1)^r t^r}{r!} \binom{r}{i} \left(\frac{\alpha}{e-1}\right)^{\frac{i}{\beta}-\frac{r}{\beta}} \Gamma\left(\frac{r}{\beta} - \frac{i}{\beta} + 1\right); \quad r = 1, 2, \cdots$$

Theorem 3.7 (Mean Residual Life (MRL) Function)**.** *The MRL function also known as the Mean Remaining Life function is another important reliability measure which provides the expected remaining lifetime given that a subject has survived up to a certain time t. For a nonnegative random variable T with survival function $S(t) = P(T > t)$ the MRL function is given by $m(t) = \mathbb{E}[T - t \mid T > t] = \frac{\int_t^\infty S(u)\,du}{S(t)}$, where $S(t) = 1 - F(t)$ is the survival function of T with $F(t)$ being the cumulative distribution function (CDF), $m(t)$ represents the mean residual life at time t or the expected remaining time beyond t given survival up to t. For the suggested ORET-L distribution, it is given as*

$$m(t) = \frac{\lambda\Gamma\left(\frac{1}{\beta}, \frac{\alpha}{e-1}\left(1+\frac{t}{\lambda}\right)^\beta\right)}{e^{-\frac{\alpha}{(e-1)}\left\{\left(1+\frac{t}{\lambda}\right)^\beta - 1\right\}}}.$$

The MRL function is widely used in reliability engineering survival analysis and actuarial science to model remaining lifetimes and assess risk over time.

Theorem 3.8 (Tail Index)**.** *The tail index of the ORET-L distribution is $\gamma = \frac{1}{\beta}$.*

Proof. To compute the tail index of the ORET-L distribution, we need to examine the asymptotic behavior of the survival function $S(x)$ as $x \to \infty$. The tail index quantifies how quickly the probability decays for large x, giving insight into the heaviness of the tail of the distribution. Starting with the CDF $F(x)$, the survival function is given by the complement of the CDF:

$$S(x) = 1 - F(x) = e^{-\frac{\alpha}{e-1}\left\{\left(1+\frac{x}{\lambda}\right)^\beta - 1\right\}}.$$

For large values of x, we analyze the behavior of the survival function by approximating $\left(1+\frac{x}{\lambda}\right)^\beta$ as $\left(\frac{x}{\lambda}\right)^\beta$, which dominates as $x \to \infty$. Hence, the survival function for large x becomes $S(x) \approx e^{-\frac{\alpha}{e-1}\left(\left(\frac{x}{\lambda}\right)^\beta - 1\right)}$. For very large x, the term $\left(\frac{x}{\lambda}\right)^\beta$ becomes much larger than 1, so we can approximate the survival function as $S(x) \approx e^{-\frac{\alpha}{e-1}\left(\frac{x^\beta}{\lambda^\beta}\right)}$. This approximation shows that the survival function decays exponentially as $x \to \infty$, and the decay rate is influenced by the parameter β. To determine the tail index γ, we compare the asymptotic behavior of $S(x)$ to a power-law decay, i.e., $S(x) \sim x^{-\gamma}$, where γ represents the tail index. Taking the logarithm of both sides, we get $\log(S(x)) \sim -\gamma \log(x)$. Now, using the asymptotic form of $S(x)$, $\log(S(x)) \sim -\frac{\alpha}{e-1}\left(\frac{x^\beta}{\lambda^\beta}\right)$. By comparing the two expressions

for $\log(S(x))$, we match the exponents of x to find that the tail index γ is related to β. Specifically, the tail index is given by $\gamma = \frac{1}{\beta}$. Therefore, for ORET-L distribution, the tail index γ is $\frac{1}{\beta}$, indicating that the survival function decays according to a power law with an exponent of $\frac{1}{\beta}$. This result characterizes the tail heaviness of the distribution.

The tail index $\gamma = \frac{1}{\beta}$ derived from ORET-L distribution suggests a Pareto-like behavior in the tail. Specifically, this tail behavior is characteristic of distributions with power-law decays in the tail. One of the standard distributions with a similar tail index is the Pareto distribution. The Pareto distribution is defined by the survival function

$$S(x) = \left(\frac{x_m}{x}\right)^{\alpha} \quad \text{for} \quad x \geq x_m,$$

where x_m is the minimum value of x (scale parameter) and α is the shape parameter, often interpreted as the tail index. For the Pareto distribution, the tail index γ is equal to the shape parameter α, which corresponds to the power-law decay rate of the survival function $S(x) \sim x^{-\alpha}$. Now, if we compare this with ORET-L distribution derived earlier where the tail index $\gamma = \frac{1}{\beta}$, it is clear that the tail of ORET-L distribution decays in a similar manner to the Pareto distribution, but with a different form for the survival function. The parameter β in ORET-L distribution plays a similar role to α in the Pareto distribution, determining the rate at which the tail of the distribution decays.

□

Figures (7-10) are the 3-dimensional plots of the Mean, Variance, Skewness and Kurtosis respectively.

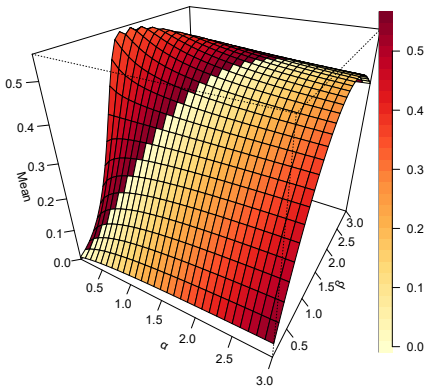

Figure 7. Mean of ORET-L

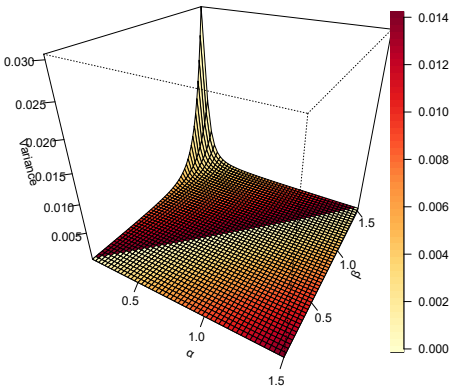

Figure 8. Variance of ORET-L

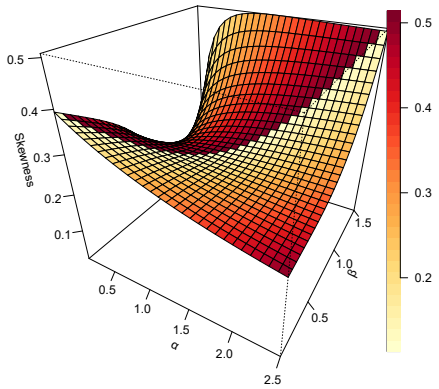

Figure 9. Skewness of ORET-L

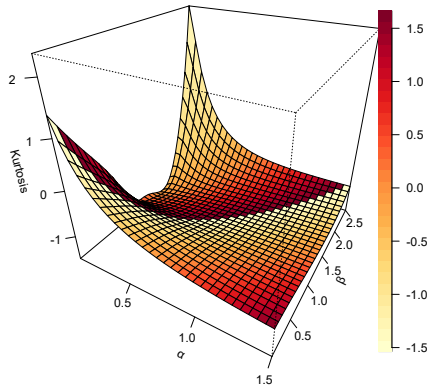

Figure 10. Kurtosis of ORET-L

4. Statistical Inference

This section addresses the parameter estimation methods for the ORET-L distribution, employing both Bayesian and classical approaches. By utilizing multiple methods, we enable a comprehensive evaluation of their respective efficiencies, particularly for large sample sizes.

4.1. Maximum Likelihood Estimation (MLE)

Suppose $x_1, x_2, \ldots, x_n$ represent a sample of n independent observations derived from the ORET-L distribution with parameters α, β, and λ. The likelihood function, denoted as $L(X|\Theta)$, along with its corresponding log-likelihood function, serves as the basis for parameter estimation. These functions are expressed as:

$$L(X|\Theta) = \left[\frac{\alpha\beta}{\lambda(e-1)}\right]^n e^{-\frac{\alpha}{e-1}\sum_{i=1}^{n}\left\{\left(1+\frac{x}{\lambda}\right)^{\beta}-1\right\}} \prod_{i=1}^{n}\left(1+\frac{x}{\lambda}\right)^{\beta-1}. \tag{10}$$

The log-likelihood function is given by:

$$\ell = n\ln\alpha + n\ln\beta - n\ln\lambda - n\ln(e-1) - \frac{\alpha}{e-1}\sum_{i=1}^{n}\left\{\left(1+\frac{x}{\lambda}\right)^{\beta}-1\right\} + (\beta-1)\sum_{i=1}^{n}\ln\left(1+\frac{x}{\lambda}\right). \tag{11}$$

To estimate α, we compute the partial derivative of ℓ with respect to α:

$$\frac{\partial\ell}{\partial\alpha} = \frac{n}{\alpha} - \frac{1}{e-1}\sum_{i=1}^{n}\left\{\left(1+\frac{x}{\lambda}\right)^{\beta}-1\right\}.$$

Setting $\frac{\partial\ell}{\partial\alpha} = 0$ yields the maximum likelihood estimate for α, expressed as:

$$\hat{\alpha} = \frac{n(e-1)}{\sum_{i=1}^{n}\left\{\left(1+\frac{x}{\lambda}\right)^{\beta}-1\right\}}. \tag{12}$$

Similarly, the partial derivative of ℓ with respect to β is:

$$\frac{\partial\ell}{\partial\beta} = \frac{n}{\beta} - \frac{\alpha}{e-1}\sum_{i=1}^{n}\left(1+\frac{x}{\lambda}\right)^{\beta}\ln\left(1+\frac{x}{\lambda}\right) + \sum_{i=1}^{n}\ln\left(1+\frac{x}{\lambda}\right). \tag{13}$$

The partial derivative of ℓ with respect to λ is:

$$\frac{\partial \ell}{\partial \lambda} = -\frac{n}{\lambda} + \frac{\alpha\beta}{\lambda^2(e-1)} \sum_{i=1}^{n} x_i \left(1 + \frac{x}{\lambda}\right)^{\beta-1} - \frac{(\beta-1)}{\lambda} \sum_{i=1}^{n} \frac{x}{\lambda + x}. \tag{14}$$

The parameters β and λ are estimated by solving equations (13) and (14) simultaneously. Due to the non-linear nature of these equations, numerical methods, such as the Newton-Raphson algorithm, are utilized to iteratively refine the parameter estimates, ensuring the maximization of the likelihood function.

4.2. Least Squares Estimation (LSE)

The Least Squares Estimation (LSE) method, first introduced by (Swain, Venkatraman, and Wilson 1988) for parameter estimation in the Beta distribution, provides the foundation for our approach. Building on their methodology, we estimate parameters by minimizing the sum of squared deviations between observed and theoretical values. This technique ensures that the distribution model closely aligns with the data, offering precise parameter estimates. By emphasizing the fit between the theoretical distribution and empirical observations, this method remains a cornerstone for reliable parameter estimation.

$$E\left[F\left(x_{j:n}|\alpha,\beta,\lambda\right)\right] = \frac{j}{n+1}; \quad \text{and} \quad V\left[F\left(x_{j:n}|\alpha,\beta,\lambda\right)\right] = \frac{j(n-j+1)}{(n+1)^2(n+2)}.$$

The parameters α, β, and λ are estimated using the Least Squares Estimation (LSE) method, producing the estimates $\hat{\alpha}_{\text{LSE}}$, $\hat{\beta}_{\text{LSE}}$, and $\hat{\lambda}_{\text{LSE}}$. These estimates are derived by minimizing the function $L(\alpha,\beta,\lambda)$ with respect to the parameters. This approach identifies parameter values that minimize the squared differences between observed and theoretical values, ensuring the model achieves the best possible fit to the data.

$$L(\alpha,\beta,\lambda) = \arg\min_{(\alpha,\beta,\lambda)} \sum_{j=1}^{n} \left[F\left(x_{j:n}|\alpha,\beta,\lambda\right) - \frac{j}{n+1}\right]^2.$$

The parameters α, β, and λ are estimated by solving a system of non-linear equations that arise from the minimization process. These equations are constructed by equating the partial derivatives of the least squares objective function $L(\alpha,\beta,\lambda)$ with respect to α, β, and λ to zero. The solutions to this system provide the Least Squares Estimators, denoted as $\hat{\alpha}_{\text{LSE}}$, $\hat{\beta}_{\text{LSE}}$, and $\hat{\lambda}_{\text{LSE}}$.

$$\sum_{j=1}^{n} \left[F\left(x_{j:n}|\alpha,\beta,\lambda\right) - \frac{j}{n+1}\right]^2 \Delta_1\left(x_{j:n}|\alpha,\beta,\lambda\right) = 0, \tag{15}$$

$$\sum_{j=1}^{n} \left[F\left(x_{j:n}|\alpha,\beta,\lambda\right) - \frac{j}{n+1}\right]^2 \Delta_2\left(x_{j:n}|\alpha,\beta,\lambda\right) = 0 \tag{16}$$

$$\sum_{j=1}^{n} \left[F\left(x_{j:n}|\alpha,\beta,\lambda\right) - \frac{j}{n+1}\right]^2 \Delta_3\left(x_{j:n}|\alpha,\beta,\lambda\right) = 0 \tag{17}$$

Where

$$\Delta_1\left(x_{j:n}|\alpha,\beta,\lambda\right) = \frac{\left(1+\frac{x}{\lambda}\right)^{\beta} - 1}{e-1} e^{-\frac{\alpha}{e-1}\left(\left(1+\frac{x}{\lambda}\right)^{\beta}-1\right)}, \tag{18}$$

$$\Delta_2\left(x_{j:n}|\alpha,\beta,\lambda\right) = \frac{\alpha}{e-1} e^{-\frac{\alpha}{e-1}\left(\left(1+\frac{x}{\lambda}\right)^{\beta}-1\right)} \cdot \ln\left(1+\frac{x}{\lambda}\right) \cdot \left(1+\frac{x}{\lambda}\right)^{\beta}, \tag{19}$$

and

$$\Delta_3(x_{j:n}|\alpha,\beta,\lambda) = \frac{\alpha}{e-1} e^{-\frac{\alpha}{e-1}\left(\left(1+\frac{x}{\lambda}\right)^{\beta}-1\right)} \cdot \beta\frac{x}{\lambda^2}\left(1+\frac{x}{\lambda}\right)^{\beta-1}. \tag{20}$$

The expressions in equations (18), (19), and (20) are derived by taking the partial derivatives of the cumulative distribution function (CDF) of the ORET-L distribution, as defined in equation (4), with respect to the parameters α, β, and λ. These derivatives form the basis for the equations used in parameter estimation, enabling an assessment of how variations in each parameter influence the CDF. This process ultimately facilitates the computation of the Least Squares Estimates for the parameters.

4.3. Weighted Least Squares Estimation (WLSE)

The Weighted Least Squares Estimation (WLSE) method is employed for parameter estimation in the ORET-L distribution, where the goal is to estimate the parameters α, β, and λ. By minimizing the weighted least squares function $W(\alpha,\beta,\lambda)$, the estimates $\hat{\alpha}_{\text{WLSE}}$, $\hat{\beta}_{\text{WLSE}}$, and $\hat{\lambda}_{\text{WLSE}}$ are obtained. Unlike standard least squares, the WLSE incorporates weights w_j to account for the varying precision of different observations. This adjustment enhances the accuracy of the parameter estimates by assigning greater weight to more reliable or relevant data points.

The weighted least squares function is given by:

$$W(\alpha,\beta,\lambda) = \arg\min_{(\alpha,\beta,\lambda)} \sum_{j=1}^{n} w_j \left[F(x_{j:n}|\alpha,\beta,\lambda) - \frac{j}{n+1}\right]^2 \tag{21}$$

where the weight w_j for each observation is defined as:

$$w_j = \frac{(n+1)^2(n+2)}{j(n-j+1)}.$$

The parameter estimates are derived by solving the following system of equations, where the weighted sums of squared deviations are equated to zero:

$$\sum_{j=1}^{n} w_j \left[F(x_{j:n}|\alpha,\beta,\lambda) - \frac{j}{n+1}\right]^2 \Delta_1(x_{j:n}|\alpha,\beta,\lambda) = 0, \tag{22}$$

$$\sum_{j=1}^{n} w_j \left[F(x_{j:n}|\alpha,\beta,\lambda) - \frac{j}{n+1}\right]^2 \Delta_2(x_{j:n}|\alpha,\beta,\lambda) = 0, \tag{23}$$

$$\sum_{j=1}^{n} w_j \left[F(x_{j:n}|\alpha,\beta,\lambda) - \frac{j}{n+1}\right]^2 \Delta_3(x_{j:n}|\alpha,\beta,\lambda) = 0. \tag{24}$$

Here, $\Delta_1(x_{j:n}|\alpha,\beta,\lambda)$, $\Delta_2(x_{j:n}|\alpha,\beta,\lambda)$, and $\Delta_3(x_{j:n}|\alpha,\beta,\lambda)$ are the partial derivatives of the cumulative distribution function (CDF) of the ORET-L distribution with respect to the parameters α, β, and λ, respectively, as defined in equations (18), (19), and (20). These derivatives are central to the computation of the weighted least squares estimates, as they describe how each parameter influences the CDF.

4.4. Maximum Product of Spacing Estimation (MPSE)

The Maximum Product of Spacing Estimation (MPSE) method, introduced by (Cheng and Amin 1979), provides an alternative to the traditional maximum likelihood estimation by focusing on the Kullback-Leibler information criterion rather than maximizing the likelihood function directly. This method is particularly useful for ordered data, as it maximizes the product of the spacings between the cumulative distribution function (CDF)

values of ordered observations. By minimizing the discrepancy between the observed and predicted distributions, the MPSE method tends to provide robust and reliable parameter estimates, especially in situations where the maximum likelihood estimation might be problematic.

The product of spacings function $P_s(X|\alpha,\beta,\lambda)$ is given by:

$$P_s(X|\alpha,\beta,\lambda) = \left[\prod_{j=1}^{n+1} D_k\big(x_{j:n}|\alpha,\beta,\lambda\big)\right]^{\frac{1}{n+1}},$$

where $D_k\big(x_{j:n}|\alpha,\beta,\lambda\big)$ represents the spacing between the CDF values of consecutive observations, defined as:

$$D_k\big(x_{j:n}|\alpha,\beta,\lambda\big) = F\big(x_j|\alpha,\beta,\lambda\big) - F\big(x_{j-1}|\alpha,\beta,\lambda\big), \quad j = 1,2,3,\ldots,n.$$

To estimate the parameters, we maximize the following function $M_s(\alpha,\beta,\lambda)$, which is the logarithm of the product of spacings:

$$M_s(\alpha,\beta,\lambda) = \frac{1}{n+1}\sum_{j=1}^{n+1} \ln\big(D_k\big(x_{j:n}|\alpha,\beta,\lambda\big)\big). \tag{25}$$

The parameter estimates are obtained by differentiating the function $M_s(\alpha,\beta,\lambda)$ with respect to α, β, and λ, and solving the resulting system of nonlinear equations:

$$\frac{\partial M_s(\alpha,\beta,\lambda)}{\partial\alpha} = 0, \quad \frac{\partial M_s(\alpha,\beta,\lambda)}{\partial\beta} = 0, \quad \frac{\partial M_s(\alpha,\beta,\lambda)}{\partial\lambda} = 0.$$

Solving this system yields the parameter estimates that maximize the product of spacings function and satisfy the given conditions.

4.5. Cramér-von Mises Estimation (CVME)

The Cramér-von Mises estimation method is used to estimate the parameters α, β, and λ of the ORET-L distribution. The estimates, denoted as $\hat{\alpha}_{\text{CVME}}$, $\hat{\beta}_{\text{CVME}}$, and $\hat{\lambda}_{\text{CVME}}$, are derived by minimizing the Cramér-von Mises criterion function $W(\alpha,\beta,\lambda)$ with respect to each parameter. This method aims to minimize the squared differences between the empirical distribution function and the theoretical cumulative distribution function, providing a robust approach for parameter estimation that better captures the model's fit to the observed data.

The Cramér-von Mises criterion function $W(\alpha,\beta,\lambda)$ is given by:

$$W(\alpha,\beta,\lambda) = \arg\min_{(\alpha,\beta,\lambda)}\left\{\frac{1}{12n} + \sum_{j=1}^{n}\left[F\big(x_{j:n}|\alpha,\beta,\lambda\big) - \frac{2j-1}{2n}\right]^2\right\}.$$

The estimates are obtained by solving the following set of non-linear equations:

$$\sum_{j=1}^{n}\left[F\big(x_{j:n}|\alpha,\beta,\lambda\big) - \frac{2j-1}{2n}\right]\Delta_1\big(x_{j:n}|\alpha,\beta,\lambda\big) = 0, \tag{26}$$

$$\sum_{j=1}^{n}\left[F\big(x_{j:n}|\alpha,\beta,\lambda\big) - \frac{2j-1}{2n}\right]\Delta_2\big(x_{j:n}|\alpha,\beta,\lambda\big) = 0, \tag{27}$$

$$\sum_{j=1}^{n}\left[F\big(x_{j:n}|\alpha,\beta,\lambda\big) - \frac{2j-1}{2n}\right]\Delta_3\big(x_{j:n}|\alpha,\beta,\lambda\big) = 0, \tag{28}$$

where $\Delta_1(x_{j:n} \mid \alpha, \beta, \lambda)$, $\Delta_2(x_{j:n} \mid \alpha, \beta, \lambda)$, and $\Delta_3(x_{j:n} \mid \alpha, \beta, \lambda)$ are defined as outlined in equations (18), (19), and (20), respectively.

4.6. Anderson-Darling Estimation (ADE)

The Anderson-Darling estimators $\hat{\alpha}_{ADE}$, $\hat{\beta}_{ADE}$, and $\hat{\lambda}_{ADE}$ for the parameters α, β, and λ of the ORET-L distribution are obtained by minimizing the function $T(\alpha, \beta, \lambda)$ with respect to α, β, and λ.

The function $T(\alpha, \beta, \lambda)$ is given by:

$$T(\alpha, \beta, \lambda) = \arg\min_{(\alpha,\beta,\lambda)} \sum_{j=1}^{n} (2j-1)\{\ln\left(F(x_{j:n}|\alpha,\beta,\lambda)\right) + \ln\left[1 - F(x_{n+1-j:n}|\alpha,\beta,\lambda)\right]\}$$

The estimates are derived by solving the following set of non-linear equations:

$$\sum_{j=1}^{n} (2j-1)\left[\frac{\Delta_1(x_{j:n}|\alpha,\beta,\lambda)}{F(x_{j:n}|\alpha,\beta,\lambda)} - \frac{\Delta_1(x_{n+1-j:n}|\alpha,\beta,\lambda)}{1 - F(x_{n+1-j:n}|\alpha,\beta,\lambda)}\right] = 0, \tag{29}$$

$$\sum_{j=1}^{n} (2j-1)\left[\frac{\Delta_2(x_{j:n}|\alpha,\beta,\lambda)}{F(x_{j:n}|\alpha,\beta,\lambda)} - \frac{\Delta_2(x_{n+1-j:n}|\alpha,\beta,\lambda)}{1 - F(x_{n+1-j:n}|\alpha,\beta,\lambda)}\right] = 0, \tag{30}$$

$$\sum_{j=1}^{n} (2j-1)\left[\frac{\Delta_3(x_{j:n}|\alpha,\beta,\lambda)}{F(x_{j:n}|\alpha,\beta,\lambda)} - \frac{\Delta_3(x_{n+1-j:n}|\alpha,\beta,\lambda)}{1 - F(x_{n+1-j:n}|\alpha,\beta,\lambda)}\right] = 0, \tag{31}$$

where $\Delta_1(x_{j:n} \mid \alpha, \beta, \lambda)$, $\Delta_2(x_{j:n} \mid \alpha, \beta, \lambda)$, and $\Delta_3(x_{j:n} \mid \alpha, \beta, \lambda)$ are defined as specified in equations (18), (19), and (20), respectively.

4.7. Right-Tailed Anderson-Darling Estimation (RTADE)

The estimates $\hat{\alpha}_{\text{RTADE}}$, $\hat{\beta}_{\text{RTADE}}$, and $\hat{\lambda}_{RTADE}$ for the parameters α, β, and λ of the ORET-L distribution, derived using the Right-Tailed Anderson-Darling method, are obtained by minimizing the function $T_r(\alpha, \beta, \lambda)$ with respect to α, β, and λ.

The function $T_r(\alpha, \beta, \lambda)$ is given by:

$$T_r(\alpha, \beta, \lambda) = \arg\min_{(\alpha,\beta,\lambda)} \left\{\frac{n}{2} - 2\sum_{j=1}^{n} F(x_{j:n}|\alpha,\beta,\lambda) - \frac{1}{n}\sum_{j=1}^{n}(2j-1)\ln\left[1 - F(x_{n+1-j:n}|\alpha,\beta,\lambda)\right]\right\}.$$

The estimates are derived by solving the following set of non-linear equations:

$$-2\sum_{j=1}^{n} \frac{\Delta_1(x_{j:n}|\alpha,\beta,\lambda)}{F(x_{j:n}|\alpha,\beta,\lambda)} + \frac{1}{n}\sum_{j=1}^{n}(2j-1)\left[\frac{\Delta_1(x_{n+1-j:n}|\alpha,\beta,\lambda)}{1 - F(x_{n+1-j:n}|\alpha,\beta,\lambda)}\right] = 0, \tag{32}$$

$$-2\sum_{j=1}^{n} \frac{\Delta_2(x_{j:n}|\alpha,\beta,\lambda)}{F(x_{j:n}|\alpha,\beta,\lambda)} + \frac{1}{n}\sum_{j=1}^{n}(2j-1)\left[\frac{\Delta_2(x_{n+1-j:n}|\alpha,\beta,\lambda)}{1 - F(x_{n+1-j:n}|\alpha,\beta,\lambda)}\right] = 0, \tag{33}$$

$$-2\sum_{j=1}^{n} \frac{\Delta_3(x_{j:n}|\alpha,\beta,\lambda)}{F(x_{j:n}|\alpha,\beta,\lambda)} + \frac{1}{n}\sum_{j=1}^{n}(2j-1)\left[\frac{\Delta_3(x_{n+1-j:n}|\alpha,\beta,\lambda)}{1 - F(x_{n+1-j:n}|\alpha,\beta,\lambda)}\right] = 0, \tag{34}$$

where $\Delta_1(x_{j:n} \mid \alpha, \beta, \lambda)$, $\Delta_2(x_{j:n} \mid \alpha, \beta, \lambda)$, and $\Delta_3(x_{j:n} \mid \alpha, \beta, \lambda)$ are defined as detailed in equations (18), (19), and (20), respectively. The estimates presented in equations (12), (13), (14), (15), (16), (17), (22), (23), (24), (25), (26), (27), (28), (29), (30), (31), (32), (33), (34) were obtained using the *optim()* function in R, which applies the Newton-Raphson iterative method.

4.8. Bayesian Estimation

This section focuses on deriving the Bayesian estimates (BE) for the unknown parameters of the ORET-L distribution. In Bayesian parameter estimation, various loss functions can be used, such as the squared error, LINEX, and generalized entropy loss functions. For parameter estimation, we assume that independent gamma priors are assigned to α, β, and λ, and the corresponding probability density functions (PDFs) form the prior distribution for the ORET-L model.

$$\left.\begin{array}{lll} \pi_1(\alpha) & \propto & \alpha^{p_1-1}e^{-q_1\alpha}, \quad \alpha>0,\ p_1>0,\ q_1>0 \\ \pi_2(\beta) & \propto & \beta^{p_2-1}e^{-q_2\beta}, \quad \beta>0,\ p_2>0,\ q_2>0 \\ \pi_3(\lambda) & \propto & \lambda^{p_3-1}e^{-q_3\lambda}, \quad \lambda>0,\ p_3>0,\ q_3>0 \end{array}\right\} \tag{35}$$

The hyperparameters p_j and q_j, for $j=1,2$, are chosen based on prior knowledge of the parameters. The joint prior distribution for $\Theta=(\alpha,\beta,\lambda)$ is expressed as follows:

$$\left.\begin{array}{ll} \pi(\Theta) & = \pi_1(\alpha)\pi_2(\beta)\pi_3(\lambda) \\ \pi(\Theta) & \propto \alpha^{p_1-1}\beta^{p_2-1}\lambda^{p_3-1}e^{-q_1\alpha-q_2\beta-q_3\lambda} \end{array}\right\} \tag{36}$$

The posterior probability distribution, conditional on the observed data $X=(x_1,x_2,\ldots,x_n)$, is represented by the following expression:

$$\pi(\Theta \mid X) = \frac{\pi(\Theta)\iota(\Theta)}{\int_\Theta \pi(\Theta)\iota(\Theta)\,d\Theta}$$

Thus, the posterior density function is:

$$\pi(\Theta \mid X) \propto \frac{\alpha^{p_1+n-1}\beta^{p_2+n-1}\lambda^{p_3-n-1}}{(e-1)^n} e^{-q_1\alpha-q_2\beta-q_3\lambda-\frac{\alpha}{e-1}\sum_{i=1}^{n}\left\{\left(1+\frac{x}{\lambda}\right)^\beta-1\right\}} \prod_{i=1}^{n}\left(1+\frac{x}{\lambda}\right)^{\beta-1}. \tag{37}$$

For any function $\vartheta(\Theta)$, the Bayes estimator under the squared error loss (SEL) criterion is given by:

$$\hat{\Theta}_{BE\_SEL} = E[\vartheta(\Theta)|x] = \int_\Theta \vartheta(\Theta)\pi(\Theta|x)d\Theta. \tag{38}$$

The squared error loss (SEL) treats underestimations and overestimations symmetrically due to its symmetric loss function. However, in real-world applications, either overestimating or underestimating may have significantly different consequences. Therefore, the LINEX loss function can be a better alternative to SEL, as described by

$$\left(\vartheta(\Theta),\hat{\vartheta}(\Theta)\right) = e^{\left\{\hat{\vartheta}(\Theta)-\vartheta(\Theta)\right\}} - \kappa\left(\hat{\vartheta}(\Theta)-\vartheta(\Theta)\right)-1,$$

where $\kappa \neq 0$ is a shape parameter. If $\kappa>1$, it indicates that overestimations are more crucial than underestimations, while $\kappa<0$ indicates the opposite. As κ approaches zero, the loss function converges to the standard squared error (SE) loss. More details on this can be found in (Varian 1975) and (Doostparast, Akbari, and Balakrishna 2011). The Bayes estimator (BE) of $\vartheta(\Theta)$ under this loss function is given by:

$$\hat{\Theta}_{\text{BE\_LINEX}} = \mathbb{E}\left[e^{-\kappa\,\vartheta(\Theta)}\,\middle|\,x\right] = -\frac{1}{\kappa}\log\left(\int_\Theta e^{-\kappa\,\vartheta(\Theta)}\,\pi(\Theta\mid x)\,d\Theta\right). \tag{39}$$

We also introduce the Generalized Entropy Loss (GEL) function, as defined by (Calabria and Pulcini 1996), which is given by:

$$(\vartheta(\Theta), \hat{\vartheta}(\Theta)) = \left(\frac{\hat{\vartheta}(\Theta)}{\vartheta(\Theta)}\right)^{-\beta} - \beta \log\left(\frac{\hat{\vartheta}(\Theta)}{\vartheta(\Theta)}\right) - 1.$$

The shape parameter $\beta \neq 0$ indicates the deviation from symmetry. When $\beta > 0$, overestimations are more critical than underestimations, while $\beta < 0$ suggests the reverse. In this case, the Bayes estimator under the GEL is computed as:

$$\hat{\Theta}_{\text{BE\_GEL}} = \mathbb{E}\left[(\vartheta(\Theta))^{-\beta} \,\middle|\, x\right]^{-1/\beta} = \left(\int_{\Theta} (\vartheta(\Theta))^{-\beta} \pi(\Theta|x)\, d\Theta\right)^{-1/\beta}. \tag{40}$$

As the estimates derived from equations (38), (39), and (39) do not have closed-form expressions, posterior samples must be generated and Bayes estimates computed using the Markov Chain Monte Carlo (MCMC) method (refer to (Brooks 1998) and (Van Ravenzwaaij, Cassey, and Brown 2018) for further details on MCMC). In MCMC, an initial batch of samples, of size N, is drawn from the posterior distribution, and a "burn-in" period is applied, discarding the first ϑ_b samples. The remaining samples are used to calculate the Bayes estimates. Using MCMC for SEL, LINEX, and GEL loss functions, the Bayes estimates $\Theta^{(j)} = (\alpha^{(j)}, \beta^{(j)}, \lambda^{(j)})$ are computed as follows:

$$\hat{\Theta}_{\text{BE\_SEL}} = \frac{1}{N - \vartheta_b} \sum_{j=\vartheta_b}^{N} \Theta(j), \tag{41}$$

$$\hat{\Theta}_{\text{BE\_LINEX}} = -\frac{1}{\kappa} \log\left(\frac{1}{N - \vartheta_b} \sum_{j=\vartheta_b}^{N} e^{-\kappa\Theta(j)}\right), \tag{42}$$

and

$$\hat{\Theta}_{\text{BE\_GEL}} = \left(\frac{1}{N - \vartheta_b} \sum_{j=\vartheta_b}^{N} \Theta(j)^{-\beta}\right)^{-\frac{1}{\beta}}, \tag{43}$$

where ϑ_b denotes the number of burn-in samples.

5. Simulation

This study applies a variety of non-Bayesian estimation methods for comparison, including Maximum Likelihood (ML), Maximum Product of Spacings (MPS), Least Squares (LS), Weighted Least Squares (WLS), Cramér-von Mises (CVM), Anderson-Darling (AD), and Right-Tail Anderson-Darling (RTAD). For each method, parameter estimates were obtained through 10,000 bootstrap samples, evaluated across four distinct sample sizes. In addition to these non-Bayesian methods, the Markov Chain Monte Carlo (MCMC) technique was employed to generate posterior samples for Bayesian estimation, as no closed-form solutions could be derived directly from equations (37), (39), and (40).

To enhance the robustness of the Bayesian estimations, a bootstrap procedure was integrated with MCMC. For each bootstrap sample, parameter estimates $\Theta^{(j)} = (\alpha^{(j)}, \beta^{(j)}, \lambda^{(j)})$ were calculated, with an initial burn-in period applied to the MCMC chain to ensure it had reached convergence. This process was repeated for each sample size ($n = 25, 75, 150, 200$), resulting in 10,000 bootstrap iterations. Bayesian estimates were subsequently derived using three distinct loss functions: squared error loss (SEL), LINEX loss, and generalized entropy loss (GEL).

Table 3. Average estimated biases and RMSEs of different estimation methods for ORET-L distribution at $(n = 25, 75, 150, 200)$ and $(\alpha = 0.200325, \beta = 0.3494375, \lambda = 1.8943205)$.

Method		$n = 25$		$n = 75$		$n = 150$		$n = 200$	
		Bias	RMSE	Bias	RMSE	Bias	RMSE	Bias	RMSE
MLE	α	0.28012	0.46612	0.14555	0.24912	0.08955	0.17055	0.05905	0.14255
	β	0.01955	0.18563	0.01645	0.12733	0.00733	0.09293	0.00663	0.08413
	λ	0.46603	0.64223	0.25503	0.34843	0.17153	0.22603	0.13653	0.17713
MPSE	α	0.18903	0.53153	0.10443	0.26003	0.06383	0.18473	0.05253	0.13993
	β	0.06153	0.18963	0.04623	0.12923	0.03133	0.10743	0.02663	0.08993
	λ	0.02253	0.58283	0.01333	0.27113	0.01163	0.17843	0.01533	0.13203
LSE	α	0.09333	0.86653	0.01903	0.35723	0.00993	0.26453	0.01213	0.22893
	β	0.01333	0.22323	0.00723	0.16143	0.00393	0.12523	0.00463	0.11243
	λ	0.31433	0.88543	0.20353	0.67253	0.18463	0.54343	0.14013	0.46253
WLSE	α	0.07143	0.55853	0.02233	0.26913	0.00643	0.18733	0.00503	0.15433
	β	0.00333	0.21053	0.00303	0.14823	0.00613	0.11593	0.00523	0.09333
	λ	0.22853	0.74893	0.10973	0.44723	0.07313	0.29053	0.04333	0.21293
CVME	α	0.09153	0.76243	0.02863	0.33823	0.00333	0.25913	0.00683	0.22353
	β	0.03383	0.23023	0.01533	0.16553	0.01663	0.13463	0.01383	0.11333
	λ	0.15833	0.86043	0.11833	0.65233	0.12043	0.52833	0.09683	0.44793
ADE	α	0.09813	0.54123	0.02843	0.26823	0.00533	0.18253	0.00133	0.15333
	β	0.00523	0.19823	0.00463	0.14043	0.01003	0.11333	0.00823	0.09493
	λ	0.06893	0.69253	0.05793	0.45153	0.05393	0.31133	0.04183	0.23753
RTADE	α	0.09943	0.62823	0.03823	0.37023	0.00223	0.30523	0.00753	0.26733
	β	0.01583	0.21523	0.00133	0.14383	0.00823	0.12593	0.00653	0.10713
	λ	0.15993	0.97833	0.12523	0.78143	0.15123	0.67243	0.13613	0.59923
BE_SEL	α	0.01353	0.22333	0.05723	0.16213	0.07823	0.13953	0.07483	0.12863
	β	0.41133	0.43423	0.34713	0.36133	0.30333	0.31253	0.26523	0.26623
	λ	1.42153	1.42023	1.36133	1.35713	1.30143	1.29893	1.23613	1.22953
BE_Linex1	α	0.00625	0.22813	0.05425	0.15901	0.07813	0.13813	0.07658	0.12613
	β	0.40913	0.42613	0.34580	0.35703	0.30513	0.31380	0.26713	0.26990
	λ	1.41175	1.41823	1.35687	1.34893	1.30017	1.29943	1.23385	1.22999
BE_Linex2	α	0.00812	0.22456	0.05312	0.15712	0.07634	0.13523	0.07523	0.12412
	β	0.41145	0.42812	0.34789	0.35912	0.30812	0.31456	0.26801	0.26889
	λ	1.41934	1.41523	1.36712	1.36123	1.31112	1.31278	1.24012	1.23589
BE_GEL1	α	0.02645	0.21235	0.05923	0.16112	0.08214	0.13756	0.07812	0.12634
	β	0.43912	0.45489	0.35934	0.37056	0.30978	0.31589	0.26856	0.27212
	λ	1.45178	1.45234	1.40789	1.40945	1.35123	1.35345	1.27823	1.28089
BE_GEL2	α	0.05623	0.20412	0.07189	0.16102	0.08823	0.14134	0.08312	0.12945
	β	0.49612	0.51845	0.38823	0.39978	0.32345	0.33189	0.27612	0.28278
	λ	1.49234	1.49378	1.48312	1.48445	1.44789	1.44856	1.37878	1.38123

Table 4. Average estimated biases and RMSEs of different estimation methods for ORET-L distribution at $(n = 25, 75, 150, 200)$ and $(\alpha = 0.100125, \beta = 0.003275, \lambda = 2.112005)$.

Method		$n = 25$		$n = 75$		$n = 150$		$n = 200$	
		Bias	RMSE	Bias	RMSE	Bias	RMSE	Bias	RMSE
MLE	α	0.27996	0.46981	0.14487	0.24978	0.08997	0.17495	0.05991	0.14465
	β	0.01889	0.18985	0.01591	0.12983	0.00685	0.09477	0.00685	0.08498
	λ	0.46989	0.64473	0.25492	0.34975	0.16986	0.22492	0.13983	0.17974
MPSE	α	0.18991	0.53455	0.10479	0.25953	0.06483	0.18485	0.05294	0.13976
	β	0.05963	0.18963	0.04477	0.13006	0.02984	0.10991	0.02677	0.08973
	λ	0.02176	0.58489	0.01282	0.27457	0.01194	0.17973	0.01483	0.13464
LSE	α	0.09487	0.86984	0.01985	0.35953	0.00992	0.26964	0.01155	0.22976
	β	0.01388	0.22475	0.00776	0.15989	0.00397	0.12467	0.00467	0.11256
	λ	0.31479	0.88955	0.20463	0.67489	0.18461	0.54988	0.13971	0.45962
WLSE	α	0.07183	0.55957	0.02297	0.26965	0.00590	0.18912	0.00477	0.15479
	β	0.00278	0.21485	0.00297	0.14974	0.00588	0.11777	0.00466	0.09485
	λ	0.22963	0.74980	0.10989	0.44956	0.07458	0.29488	0.04456	0.21978
CVME	α	0.08981	0.76453	0.02869	0.33965	0.00289	0.25972	0.00680	0.22496
	β	0.03363	0.22982	0.01481	0.16972	0.01688	0.13486	0.01371	0.11479
	λ	0.15976	0.86492	0.11953	0.65470	0.11952	0.52988	0.09689	0.44977
ADE	α	0.09987	0.54471	0.02979	0.26928	0.00498	0.18462	0.00095	0.15475
	β	0.00489	0.19991	0.00495	0.13955	0.00991	0.11465	0.00787	0.09479
	λ	0.06891	0.69495	0.05786	0.45479	0.05389	0.31485	0.04178	0.23988
RTADE	α	0.09977	0.62985	0.03773	0.37451	0.00192	0.30969	0.00681	0.26941
	β	0.01563	0.21972	0.00097	0.14487	0.00786	0.12995	0.00584	0.10983
	λ	0.15975	0.97991	0.12483	0.78472	0.15087	0.67492	0.13576	0.59981
BE_SEL	α	0.01289	0.22458	0.05684	0.15923	0.07752	0.13921	0.07494	0.12931
	β	0.40978	0.43492	0.34974	0.36455	0.30487	0.31484	0.26914	0.26977
	λ	1.03952	1.00941	0.90471	0.88937	0.87460	0.87443	0.85438	0.85993
BE_Linex1	α	0.00619	0.22799	0.05413	0.15876	0.07701	0.13787	0.07546	0.12597
	β	0.40897	0.42594	0.34565	0.35687	0.30504	0.31364	0.26683	0.27467
	λ	1.03901	0.99841	0.90115	0.88757	0.86871	0.87391	0.84839	0.85376
BE_Linex2	α	0.01723	0.23789	0.05523	0.16245	0.07689	0.14201	0.07712	0.13056
	β	0.41223	0.43012	0.34678	0.35912	0.30612	0.31645	0.26778	0.27056
	λ	1.42312	1.41978	1.36412	1.36356	1.30423	1.30712	1.23012	1.23212
BE_GEL1	α	0.02714	0.21468	0.04187	0.15743	0.05456	0.14145	0.05892	0.12899
	β	0.41232	0.42647	0.34780	0.35872	0.30765	0.31643	0.26812	0.27565
	λ	1.40976	1.40123	1.35056	1.36003	1.29242	1.29511	1.22542	1.22689
BE_GEL2	α	0.05798	0.20604	0.07361	0.16258	0.08954	0.14279	0.08462	0.13022
	β	0.49784	0.51942	0.38971	0.40185	0.32421	0.33310	0.27739	0.28461
	λ	1.49412	1.49568	1.48479	1.48611	1.44913	1.45002	1.38094	1.38297

Tables (3) and (4) show the performance of both non-Bayesian and Bayesian estimation methods, with emphasis on bias and Root Mean Squared Error (RMSE) across different sample sizes $n = 25, 50, 100, 200$. The parameters of the ORET-L distribution for estimation are α, β, and λ.

a For the non-Bayesian methods (MLE, MPSE, LSE, WLSE, CVME, ADE, RTADE), the bias generally decreases as the sample size increases. This is consistent with the expected behavior of estimators improving with larger sample sizes. For each parameter (α, β, λ), as n moves from 25 to 200, the bias tends to shrink, indicating that these methods become more accurate with larger data.

b The RMSE shows a similar decreasing trend as the sample size increases, reflecting more precise estimates with larger samples. This is expected for most standard estimation methods, where larger sample sizes lead to more stable and less variable estimates.

The Bayesian methods include SEL, Linex1, Linex2, GEL1, and GEL2. The performance of these methods differs from the non-Bayesian ones in the following ways:

i The Bayesian methods show relatively lower bias for both α and β compared to the non-Bayesian methods, particularly at larger sample sizes. The bias tends to stabilize and does not show substantial improvement as the sample size increases.

This suggests that the Bayesian methods provide more consistent estimates with smaller biases, even for smaller sample sizes.

ii For λ, the bias shows a slight increase with larger sample sizes in some Bayesian methods (e.g., SEL, Linex1, Linex2), but the increase is marginal compared to the non-Bayesian methods.

iii The RMSE for Bayesian methods remains relatively low across all sample sizes, particularly for α and β. This suggests that Bayesian methods tend to provide more reliable estimates with less variability as the sample size increases, indicating the robustness of Bayesian estimation.

In comparing the non-Bayesian and Bayesian methods

1. Non-Bayesian methods (such as MLE and MPSE) show significant improvements in both bias and RMSE as the sample size grows, while Bayesian methods maintain a relatively stable performance with less dramatic improvement with increasing sample size. This indicates that the Bayesian methods provide more consistent and stable estimates, even for smaller sample sizes, compared to the non-Bayesian methods.
2. Despite the bias not decreasing substantially as the sample size increases, the RMSE tends to stabilize and remain lower for Bayesian methods. This shows that the Bayesian framework provides robust and stable estimates across different sample sizes.

In summary, the Bayesian methods generally outperform the non-Bayesian methods in terms of bias, especially for α and β. Both groups exhibit reductions in RMSE with increasing sample sizes. The Bayesian methods provide more stable and less biased estimations, making them more reliable for smaller sample sizes, while the non-Bayesian methods improve more rapidly as sample size increases.

6. Application

The first dataset represents premature deaths attributed to exposure to fine particulate matter (PM2.5) in Europe from 2006 to 2021. This dataset was obtained from the European Environment Agency's website, accessible at https://www.eea.europa.eu/en/analysis/indicators/h impacts-of-exposure-to, and was retrieved on November 11, 2024. Table (5) below presents the dataset, which captures annual mortality figures associated with PM2.5 exposure across various regions in Europe over the 15-year period. Initial insights into the data are summarized in Table (6), revealing a dataset characterized by a platykurtic distribution, which is less peaked than the normal distribution, and a positive skew, indicating a longer right tail. Additionally, no distinct outliers were identified, suggesting that the values are fairly consistent over the observed years. To evaluate the performance of different statistical models on this dataset, several model selection criteria were employed. These included the negative log-likelihood (NLL), Akaike Information Criterion (AIC), Consistent AIC (CAIC), Bayesian Information Criterion (BIC), Hannan-Quinn Information Criterion (HQIC), Cramér-von Mises statistic (W), and Anderson-Darling statistic (A). For assessing goodness-of-fit, we used the Kolmogorov-Smirnov (KS) statistic and its associated probability value (p-value). These metrics provided a comprehensive framework for comparing the proposed Odd-Ratio Exponential Lomax (ORET-L) model to competing models, namely the Lomax distribution, Exponential distribution, log-normal (LNORM) distribution, and gamma distribution. The results in Table (7), indicate that the ORET-L model exhibits a superior fit to the PM2.5 data, consistently achieving the lowest values across the performance metrics. This indicates that the ORET-L model offers a more accurate representation of the data compared to the other models. In addition to the analytical results, a range of parametric and non-parametric plots were generated to visually assess the fit of the models.

Figure (11) includes several key plots: the density function superimposed on the histogram of the dataset, Probability-Probability (P-P) plot, Cumulative Distribution Function (CDF) plot, and Total Time on Test (TTT) plot. These visualizations further support the analytical findings, illustrating the strong fit of the ORET-L model to the PM2.5 data.

Table 5. Premature deaths due to exposure to fine particulate matter (PM2.5) in Europe (Data-I)

431114	349416	354207	362841	367732	392315	344027	328912
290933	321094	281995	303487	290716	231286	237715	253305

Table 6. Summary Statistics for Data-I

$\bar{X}$	S^2	S	Min	Max	IQR	Sk	Ku	S_e	Range
32.132	31.243	5.590	23.129	43.111	6.783	0.067	2.336	1.4	19.98

Table 7. Goodness of fit test and Model Performance for Data-I

Distribution	NLL	AIC	CAIC	BIC	HQIC	W	A	KS	p-value	$\hat{\alpha}_{\text{MLE}}$ (scale)	$\hat{\beta}_{\text{MLE}}$ (shape)	$\hat{\lambda}_{\text{MLE}}$ (scale)
ORET-L	69.55	108.537	110.537	110.854	108.055	0.028	0.245	0.156	0.7758	8.1748×10^{-3}	7.679×10^{5}	4.931×10^{6}
Lomax	71.52	147.035	147.958	148.580	147.114	0.029	0.200	0.513	0.0002	-	18.962	60.929
Exponential	71.52	145.035	145.321	145.808	145.075	0.029	0.200	0.513	0.0002	0.0311	-	-
LNORM	49.82	111.237	112.160	112.782	111.316	0.034	0.230	0.345	0.033	3.323	0.205	-
Gamma	49.73	112.271	113.194	113.816	112.350	0.029	0.200	0.187	0.5689	9.846	3.312	-

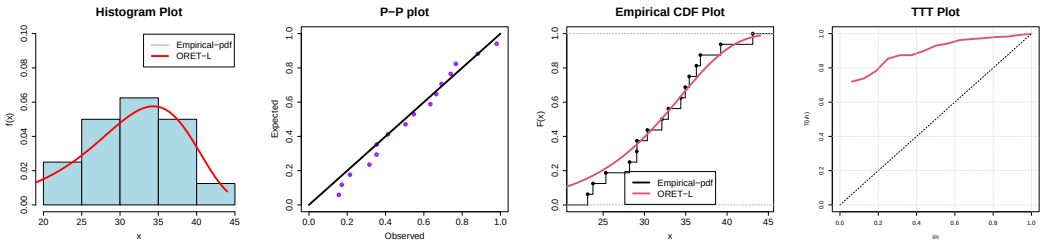

Figure 11. Parametric and non-parametric plots for Data-I

The second data obtained from (Quesenberry and Hales 1980) represent the observed tensile strength of polyester presented in Table (8) below.

Table 8. Tensile strength observations of poly-ester fibers (Data-II)

0.023	0.032	0.054	0.069	0.081	0.094	0.105	0.127
0.148	0.169	0.188	0.216	0.255	0.277	0.311	0.361
0.376	0.395	0.432	0.463	0.481	0.519	0.529	0.567
0.642	0.674	0.752	0.823	0.887	0.926		

Table 9. Summary Statistics for Data-II

$\bar{X}$	S^2	S	Min	Max	IQR	Sk	Ku	S_e	Range
0.3659	0.0721	0.2685	0.0230	0.9260	0.3943	0.5464	2.2294	0.0500	0.9000

Table 10. Goodness of fit test and Model Performance for Data-II

Distribution	NLL	AIC	CAIC	BIC	HQIC	W	A	KS	p-value	$\hat{\alpha}_{\text{MLE}}$ (scale)	$\hat{\beta}_{\text{MLE}}$ (shape)	$\hat{\lambda}_{\text{MLE}}$ (scale)
ORET-L	2.39	1.109	2.032	5.312	2.454	0.021	0.165	0.074	0.9924	1.5283	3.6008×10^{6}	2.0591×10^{6}
Lomax	0.16	3.671	4.115	6.473	4.567	0.045	0.287	0.127	0.6700	28794956	10534919	
Exponential	0.16	1.671	1.814	3.072	2.119	0.450	0.287	0.127	0.6701	2.7332		
Log-normal	-0.79	40.177	40.621	42.979	41.074	0.104	0.643	0.534	1.59×10^{-8}	0.0735	1.7530	
Gamma	1.44	1.478	1.922	4.280	2.375	0.044	0.284	0.144	0.5172	1.4261	0.2353	

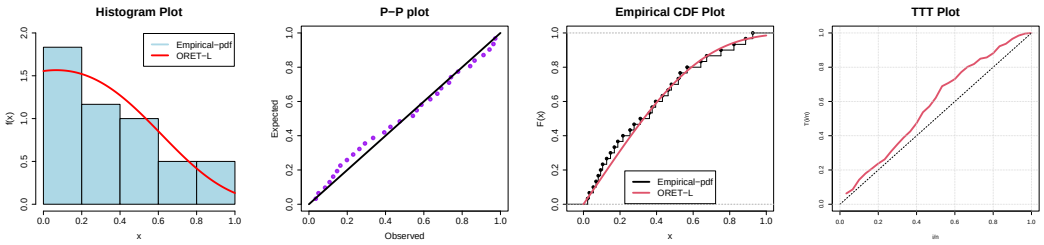

Figure 12. Parametric and non-parametric plots for Data-II

Table (9) summarizes key statistical metrics for Data-II:

(a.) The mean tensile strength ($\bar{X}$) is 0.3659, with a standard deviation (S) of 0.2685, indicating moderate variability in the dataset.

(b.) The minimum and maximum values are 0.0230 and 0.9260, respectively, giving a range of 0.9000.

(c.) The interquartile range (IQR) of 0.3943 highlights the spread of the middle 50% of observations.

(d.) The skewness (Sk) of 0.5464 suggests a slight positive skew, indicating more values are concentrated towards the lower end of the scale.

(e.) The kurtosis (Ku) of 2.2294 is close to 3, suggesting the data has nearly normal-tailed behavior.

The goodness-of-fit results in Table (10) reveal key insights:

(a.) The ORET-L distribution performs well, with a p-value of 0.9924, suggesting a good fit to the data. The estimated scale ($\hat{\alpha}$), shape ($\hat{\beta}$), and additional scale parameter ($\hat{\lambda}$) demonstrate its flexibility.

(b.) The Exponential distribution has a reasonable fit with a p-value of 0.6701 but lacks the flexibility of other models in capturing data characteristics.

(c.) The Gamma distribution also performs moderately well with a p-value of 0.5172.

(d.) The Log-normal distribution, despite its capability to model positively skewed data, shows a poor fit with a p-value of 1.59×10^{-8}.

(e.) The Lomax distribution yields a relatively weaker fit compared to the ORET-L model but remains a viable candidate for modeling the data.

The model selection criteria (e.g., AIC, BIC) align with these observations, where lower values indicate better model performance. The ORET-L distribution exhibits competitive performance across these metrics.

Figure 12 provides visual validation of the model fit:

(a.) Density Plot: The parametric and non-parametric density estimates align well for the ORET-L and other competitive models like Gamma, indicating they effectively capture the underlying data distribution.

(b.) P-P Plot: The ORET-L model closely follows the diagonal, suggesting a good agreement between observed and expected probabilities.

(c.) Empirical CDF: The ORET-L and Gamma models overlay well with the empirical cumulative distribution function (CDF), reinforcing their suitability.

(d.) TTT Plot: The Total Time on Test (TTT) plot supports the chosen models by reflecting the behavior of the underlying distribution.

The analysis highlights the versatility of the ORET-L distribution, which not only achieves a statistically significant fit but also demonstrates flexibility in capturing the characteristics of the tensile strength data. The Exponential and Gamma distributions serve as simpler alternatives, but their performance is somewhat inferior. The Log-normal distribution, while theoretically appropriate for positively skewed data, struggles to represent the

observed values effectively. Therefore, the ORET-L distribution emerges as the most appropriate model for Data-II, offering both statistical and practical alignment with the observed tensile strength of polyester fibers. The visual and statistical metrics consistently validate its superiority over competing distributions.

7. Concluding Remarks

In this study, we developed and examined a new class of weighted $T-X$ distributions, focusing on modeling fine particulate matter (PM2.5) hazards, which pose significant health and environmental risks and the tensile strength of polyester. By constructing the Odd Reparametrized Exponential Transformed-X (ORET-X) family of distributions, we created a flexible model suitable for fitting data with characteristics similar to PM2.5 exposure and tensile strength of polyester, including heavy tails and a gradual decay in event rates over time. The ORET-X family, through reparametrization, effectively captures nuances in PM2.5 concentration data as well as the observed tensile strength of polyester and introduces an adaptable hazard function that can accommodate various shapes depending on the distribution of interest. The ORET-X model was further extended to the Odd Reparametrized Exponential Transformed-Lomax (ORET-L) distribution, offering an enhanced approach to modeling heavy-tailed environmental hazards like PM2.5 and reliability data such as the observed tensile strength of poly-ester. Through this distribution, we applied both non-Bayesian and Bayesian estimation techniques to assess parameter accuracy and reliability. The non-Bayesian methods showed significant improvements in bias and Root Mean Squared Error (RMSE) with larger sample sizes, confirming the estimator consistency with sample size increase. In contrast, Bayesian estimation methods, particularly under prior choices suited to the parameter space, exhibited stability and low RMSE even at smaller sample sizes, highlighting the Bayesian framework's robustness in estimating model parameters accurately. This modeling framework for PM2.5 and tensile strength of polyester data not only addresses the immediate need for a flexible and robust hazard modeling tool but also provides a foundation for exploring further extensions. By offering a comprehensive set of parameter estimation approaches, this work demonstrates the practical applicability of the ORET-X family in environmental modeling contexts. Future studies can build upon this by exploring alternative parent distributions within the ORET-X structure, potentially expanding its applicability across various environmental and biomedical hazards with similar distributional properties.

Author Contributions: Conceptualization, G.O.O. and H.O.E.; methodology, G.O.O.; software, G.O.O.; validation, G.O.O., H.O.E. and O.J.O.; formal analysis, G.O.O.; investigation, G.O.O.; resources, G.O.O.; data curation, G.O.O.; writing—original draft preparation, G.O.O.; writing—review and editing, G.O.O.; visualization, G.O.O.; supervision, G.O.O.; project administration, G.O.O.; funding acquisition, H.O.E. All authors have read and agreed to the published version of the manuscript.

Funding: This research received no external funding.

Data Availability Statement: The data used in this study are included in the article

Conflicts of Interest: The authors declare no conflicts of interest.

References

Agarwal, Bhagwan D., Lawrence J. Broutman, and K. Chandrashekhara. 2017. *Analysis and performance of fiber composites.* John Wiley & Sons.

Al-Marzouki, Sanaa, Farrukh Jamal, Christophe Chesneau, and Mohammed Elgarhy. 2019. Type II Topp Leone power Lomax distribution with applications. *Mathematics* 8 (1): 4.

Al-Shomrani, Ali, Osama Arif, A. Shawky, Saman Hanif, and Muhammad Qaiser Shahbaz. 2016. Toppâ€"Leone Family of Distributions: Some Properties and Application. *Pakistan Journal of Statistics and Operation Research* 12: 443–51.

Alizadeh, Morad, Gauss M. Cordeiro, Luis Gustavo Bastos Pinho, and Indranil Ghosh. 2017. The Gompertz-G family of distributions. *Journal of statistical theory and practice* 11: 179–207.

Alizadeh, Mojtaba, S.F. Bagheri, E. Bahrami Samani, Saeid Ghobadi, and S. Nadarajah. 2018. Exponentiated power Lindley power series class of distributions: Theory and applications. *Communications in Statistics-Simulation and Computation* 47 (9): 2499–2531.

Almarashi, Abdullah M., Majdah M. Badr, Mohammed Elgarhy, Farrukh Jamal, and Christophe Chesneau. 2020. Statistical inference of the half-logistic inverse Rayleigh distribution. *Entropy* 22 (4): 449.

Alzaatreh, Ayman, Carl Lee, and Felix Famoye. 2013. A new method for generating families of continuous distributions. *Metron* 71 (1): 63–79.

Alzaatreh, Ayman, Carl Lee, and Felix Famoye. 2014. T-normal family of distributions: a new approach to generalize the normal distribution. *Journal of Statistical Distributions and Applications* 1: 1–18.

Alyami, Salem A., Ibrahim Elbatal, Naif Alotaibi, Ehab M. Almetwally, Hassan M. Okasha, and Mohammed Elgarhy. 2022. Topp–Leone modified Weibull model: Theory and applications to medical and engineering data. *Applied Sciences* 12 (20): 10431.

Anyiam, Kizito E., Fatimah M. Alghamdi, Chrysogonus C. Nwaigwe, Hassan M. Aljohani, and Okechukwu J. Obulezi. 2024. A new extension of Burr-Hatke exponential distribution with engineering and biomedical applications. *Heliyon* 10 (19).

Anzagra, Lea, Solomon Sarpong, and Suleman Nasiru. 2022. Odd Chen-G family of distributions. *Annals of Data Science* 9 (2): 369–91.

Baley, Christophe. 2002. Analysis of the flax fibres tensile behaviour and analysis of the tensile stiffness increase. *Composites Part A: Applied Science and Manufacturing* 33 (7): 939–48.

Bledzki, A.K., and Jochen Gassan. 1999. Composites reinforced with cellulose based fibres. *Progress in polymer science* 24 (2): 221–74.

Bourguignon, Marcelo, Rodrigo B. Silva, Luz M. Zea, and Gauss M. Cordeiro. 2013. The kumaraswamy Pareto distribution. *Journal of statistical theory and applications* 12 (2): 129–44.

Brook, Robert D., Sanjay Rajagopalan, C. Arden Pope III, Jeffrey R. Brook, Aruni Bhatnagar, Ana V. Diez-Roux, Fernando Holguin, Yuling Hong, Russell V. Luepker, Murray A. Mittleman, et al. 2010. Particulate matter air pollution and cardiovascular disease: an update to the scientific statement from the American Heart Association. *Circulation* 121 (21): 2331–78.

Brooks, Stephen. 1998. Markov chain Monte Carlo method and its application. *Journal of the royal statistical society: series D (the Statistician)* 47 (1): 69–100.

Calabria, R., and G. Pulcini. 1996. Point estimation under asymmetric loss functions for left-truncated exponential samples. *Communications in Statistics-Theory and Methods* 25 (3): 585–600.

Calderón-Garcidueñas, Lilian, Biagio Azzarelli, Hilda Acuna, Raquel Garcia, Todd M. Gambling, Norma Osnaya, Sylvia Monroy, Maria Del Rosario Tizapantzi, Johnny L. Carson, Anna Villarreal-Calderon, et al. 2002. Air pollution and brain damage. *Toxicologic pathology* 30 (3): 373–89.

Cheng, R., and N. Amin. 1979. Maximum product of spacings estimation with application to the lognormal distribution (Mathematical Report 79-1). Cardiff: University of Wales IST.

Chowdhury, Sourangsu, Andrea Pozzer, Andy Haines, Klaus Klingmueller, Thomas Münzel, Pauli Paasonen, Arushi Sharma, Chandra Venkataraman, and Jos Lelieveld. 2022. Global health burden of ambient PM2. 5 and the contribution of anthropogenic black carbon and organic aerosols. *Environment International* 159: 107020.

Cordeiro, Gauss M., and Mário De Castro. 2011. A new family of generalized distributions. *Journal of statistical computation and simulation* 81 (7): 883–98.

Cordeiro, Gauss M., Morad Alizadeh, and Pedro Rafael Diniz Marinho. 2016. The type I half-logistic family of distributions. *Journal of Statistical Computation and Simulation* 86 (4): 707–28.

Doostparast, Mahdi, Mohammad Ghasem Akbari, and N. Balakrishna. 2011. Bayesian analysis for the two-parameter Pareto distribution based on record values and times. *Journal of Statistical Computation and Simulation* 81 (11): 1393–1403.

Ekemezie, Divine-Favour N., Fatimah M. Alghamdi, Hassan M. Aljohani, Fathy H. Riad, M.M. Abd El-Raouf, and Okechukwu J. Obulezi. 2024. A more flexible Lomax distribution: Characterization, estimation, group acceptance sampling plan and applications. *Alexandria Engineering Journal* 109: 520–31.

Elbatal, I., and M. Elgarhy. 2013. Statistical properties of Kumaraswamy quasi Lindley distribution. *International Journal of Mathematics Trends and Technology-IJMTT* 4.

Elbatal, Ibrahim, Naif Alotaibi, Ehab M. Almetwally, Salem A. Alyami, and Mohammed Elgarhy. 2022. On odd perks-G class of distributions: properties, regression model, discretization, Bayesian and non-Bayesian estimation, and applications. *Symmetry* 14 (5): 883.

Gomes-Silva, Frank S., Ana Percontini, Edleide de Brito, Manoel W. Ramos, Ronaldo Venâncio, and Gauss Moutinho Cordeiro. 2017. The odd Lindley-G family of distributions. *Austrian journal of statistics* 46 (1): 65–87.

Guttikunda, Sarath K., Sereeter Lodoysamba, Baldorj Bulgansaikhan, and Batdorj Dashdondog. 2013. Particulate pollution in Ulaanbaatar, Mongolia. *Air Quality, Atmosphere & Health* 6: 589–601.

Hassan, Amal S., and Said G. Nassr. 2019. Power Lindley-G family of distributions. *Annals of Data Science* 6: 189–210.

Hearle, John W.S., and William Ernest Morton. 2008. *Physical properties of textile fibres*. Elsevier.

Jafari, Ali Akbar, and Saeid Tahmasebi. 2016. Gompertz-power series distributions. *Communications in Statistics-Theory and Methods* 45 (13): 3761–81.

Jamal, Farrukh, Christophe Chesneau, and Mohammed Elgarhy. 2020. Type II general inverse exponential family of distributions. *Journal of Statistics and Management Systems* 23 (3): 617–41.

Lehmann, Erich Leo. 2011. Ordered families of distributions. In *Selected Works of EL Lehmann*, 757–77. Springer.

Li, Meng, Zbigniew Klimont, Qiang Zhang, Randall V. Martin, Bo Zheng, Chris Heyes, Janusz Cofala, Yuxuan Zhang, and Kebin He. 2018. Comparison and evaluation of anthropogenic emissions of SO 2 and NO x over China. *Atmospheric Chemistry and Physics* 18 (5): 3433–56.

Lomax, Kenneth S. 1954. Business failures: Another example of the analysis of failure data. *Journal of the American statistical association* 49 (268): 847–52.

Mansoor, M., Gauss M. Cordeiro, and M. Zubair. 2020. A Study of the Logistic Exponentiated-exponential distribution and Its Applications. *Journal of Advances in Applied & Computational Mathematics* 7: 38–48.

Maurya, Sandeep Kumar, and Saralees Nadarajah. 2021. Poisson generated family of distributions: a review. *Sankhya B* 83: 484–540.

Nolla Solé, Joan Miquel, et al. 2012. A comparative risk assessment of burden of disease and injury attributable to 67 risk factors and risk factor clusters in 21 regions, 1990-2010: a systematic analysis for the Global Burden of Disease Study 2010. *The Lancet, 2012, vol. 380, num. 9859, p. 2224-2260* 380 (9859): 2224–60.

Okubo, Kazuya, Toru Fujii, and Yuzo Yamamoto. 2004. Development of bamboo-based polymer composites and their mechanical properties. *Composites Part A: Applied science and manufacturing* 35 (3): 377–83.

Oramulu, Dorathy O., Najwan Alsadat, Anoop Kumar, Mahmoud Mohamed Bahloul, and Okechukwu J. Obulezi. 2024. Sine generalized family of distributions: Properties, estimation, simulations and applications. *Alexandria Engineering Journal* 109: 532–52.

Pope III, C. Arden, and Douglas W. Dockery. 2006. Health effects of fine particulate air pollution: lines that connect. *Journal of the air & waste management association* 56 (6): 709–42.

Quesenberry, Charles P., and Craige Hales. 1980. Concentration bands for uniformity plots. *Journal of Statistical Computation and Simulation* 11 (1): 41–53.

Seinfeld, John H., and Spyros N. Pandis. 2016. *Atmospheric chemistry and physics: from air pollution to climate change*. John Wiley & Sons.

Shannon, Claude Elwood. 1948. A mathematical theory of communication. *The Bell system technical journal* 27 (3): 379–423.

Swain, James J., Sekhar Venkatraman, and James R. Wilson. 1988. Least-squares estimation of distribution functions in Johnson's translation system. *Journal of Statistical Computation and Simulation* 29 (4): 271–97.

Tahir, M.H., Gauss M. Cordeiro, Ayman Alzaatreh, M. Mansoor, and M. Zubair. 2016. The logistic-X family of distributions and its applications. *Communications in statistics-Theory and methods* 45 (24): 7326–49.

Tolba, Ahlam H., Chrisogonus K. Onyekwere, Ahmed R. El-Saeed, Najwan Alsadat, Hanan Alohali, and Okechukwu J. Obulezi. 2023. A New Distribution for Modeling Data with Increasing Hazard Rate: A Case of COVID-19 Pandemic and Vinyl Chloride Data. *Sustainability* 15 (17): 12782.

Van Ravenzwaaij, Don, Pete Cassey, and Scott D. Brown. 2018. A simple introduction to Markov Chain Monte–Carlo sampling. *Psychonomic bulletin & review* 25 (1): 143–54.

Varian, Hal R. 1975. A Bayesian approach to real estate assessment. *Studies in Bayesian econometrics and statistics in honor of Leonard J. Savage*. North-Holland.

Weibull, Waloddi. 1939. A statistical theory of strength of materials. *IVB-Handl.*.

Wilson, E.B. 1914. *Variabilità e Mutabilità*. JSTOR.

Yousof, Haitham M., Emrah Altun, Thiago G. Ramires, Morad Alizadeh, and Mahdi Rasekhi. 2018. A new family of distributions with properties, regression models and applications. *Journal of Statistics and Management Systems* 21 (1): 163–88.